

Impact of surficial factors on groundwater quality for irrigation using spatial techniques: emerging evidence from the northeast region of Ghana

Prosper Kpiebaya ^{a,*}, Abdul-Ganiyu Shaibu ^a, Ebenezer Ebo Yahans Amuah^b, Raymond Webrah Kazapoe ^c, Eliasu Salifu ^a and Benjamin Wullobayi Dekongmen^d

^a University for Development Studies – Nyankpala Campus, Tamale, Ghana 1882, Ghana

^b Department of Environmental Science, Kwame Nkrumah University of Science and Technology, Kumasi, Ghana, Ghana

^c Department of Geological Engineering, School of Engineering, University for Development Studies, P. O. Box TL 1350, Tamale, Ghana, Ghana

^d Department of Agricultural Engineering, Ho Technical University, P. O. Box HP 217, Ho, Ghana, Ghana

*Corresponding author. E-mail: Kpiebayaprosp@gmail.com

 PK, 0000-0002-4794-5314; A-GS, 0000-0001-6431-8083; RWK, 0000-0002-0307-7834; ES, 0000-0002-7377-3317

ABSTRACT

The need for quality water in Africa for agriculture cannot be overemphasized amidst the current global water crises. The focus of this study sought to evaluate the quality of groundwater for irrigation purposes while unearthing the emerging challenges in the study area. In total, 202 groundwater samples were collected, and several parameters were tested. The study employed QGIS and multi-criteria decision analysis to examine zones of suitable groundwater quality for agriculture. Findings from the study indicate that the primary water types were Na–HCO₃ and Ca–HCO₃. The overall accuracy (OV) of the land use land cover (LULC) map using the Random Forest (RF) algorithm was 94.5%. The analysis revealed that SpH influences GpH at $p = 0.02891$ ($p < 0.05$) and SOM and SOC influence GNO₃ at $p = 0.044$ ($p < 0.05$). The overlay analysis spatially classified the groundwater in the study area into three categories of suitability with ariel coverage showing areas of good quality (1,534.34 km²), moderate quality (1,933.35 km²), and poor quality (1,815.21 km²). The results from this study uncovered that 72.33% of the samples were within the desirable limits and it can be concluded that the quality of groundwater in the area is acceptable for irrigation.

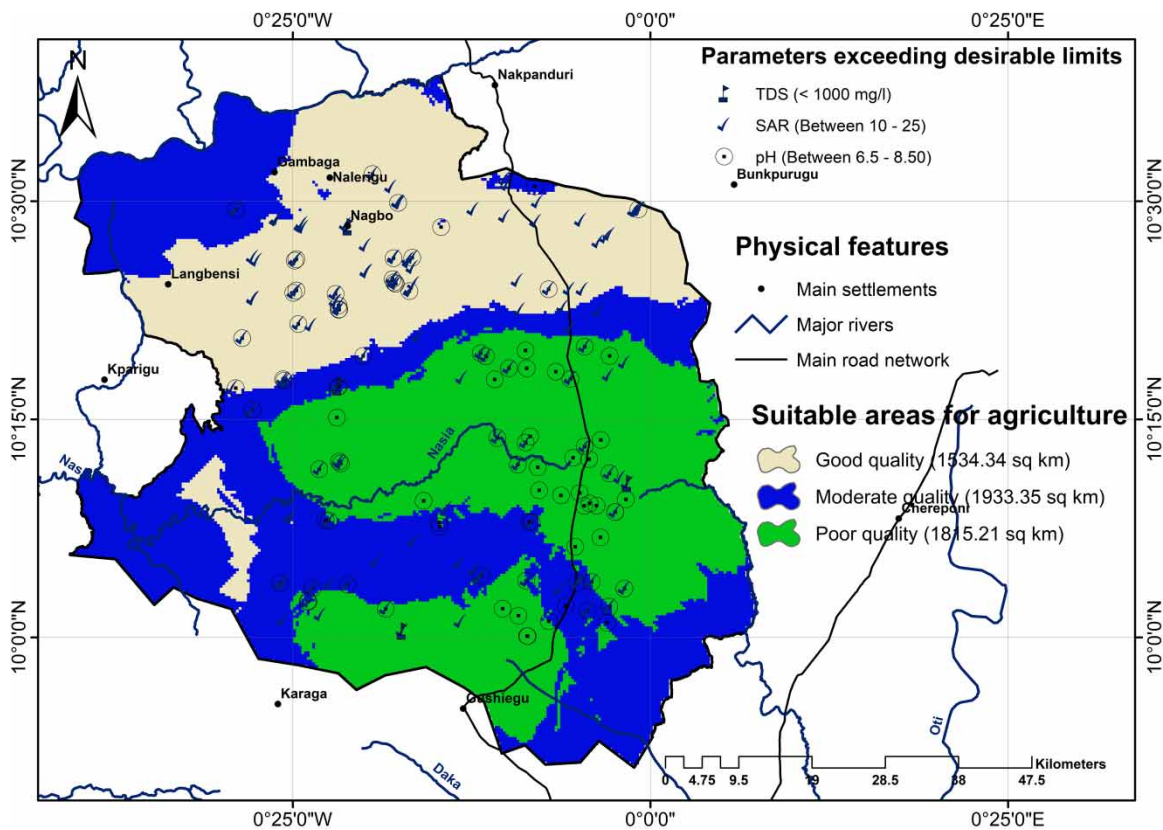
Key words: irrigation, modeling, QGIS, Savannah, spatial, water quality

HIGHLIGHTS

- This paper examines different surficial factors.
- This study presents several cases (quality versus LULC, slope, and soil).
- The paper examines the suitable areas for irrigation as per the available groundwater quality.

This is an Open Access article distributed under the terms of the Creative Commons Attribution Licence (CC BY 4.0), which permits copying, adaptation and redistribution, provided the original work is properly cited (<http://creativecommons.org/licenses/by/4.0/>).

GRAPHICAL ABSTRACT



1. INTRODUCTION

Groundwater is an essential resource, but its availability for domestic, irrigation, and industrial uses has been jeopardized by several factors, the most serious of which is climate variability (Havril *et al.* 2018). Several factors such as subsurface geochemical processes, precipitation, recharge water, and inland surface water contribute to the occurrence of poor groundwater quality (Chegbeleh *et al.* 2020). The quality of groundwater has attracted global attention due to the high-quality water demand for domestic and irrigation purposes. Groundwater quality parameters are classified into three types: physicochemical parameters, bacteriological parameters, and trace metals.

In the increasing communities of sub-Saharan Africa (SSA), groundwater usage has increased significantly for both irrigation and household use since the 1980s (Giordano 2006). Despite the huge global interest in developing groundwater for various uses within the sub-Saharan terrain, there remains a growing concern about the immediate quality. Because of this interest, routine quality analysis is required to determine suitability for consumption and irrigation purposes in Ghana, Africa, SSA, and the world at large.

In the last three decades, approximately 14,500 boreholes were drilled throughout the Northern-Voltaian belt of Ghana, with nearly 52% serving the rural population (Abdul-Ganiyu & Prosper 2021). The remaining 48% are unserviceable and can be attributed to poor quality and quantity. However, more boreholes have been drilled recently as the Ghana government has put in efforts to meet the Sustainable Development Goals (SDGs) 6 and 14 by providing clean and potable water to inaccessible communities. The question now is why some rural communities lack access to quality water and why some irrigation schemes have failed. These can be associated with the lack of data on viable areas to explore, lack of awareness, fragmented data, and lack of geospatial research on groundwater quality in the study area. For that reason, this study fundamentally aims to assess the quality of groundwater using geospatial and statistical methods following past studies while developing new methods for future use (Gidey 2018; Moharir *et al.* 2019; Rawat *et al.* 2019).

Adimalla *et al.* (2020) evaluated the quality of groundwater for drinking and irrigation purposes in Central Telangana, India. It was found that 96% of the samples were within the required quality standards and, therefore,

were recommended for irrigation. The absence of a groundwater quality suitability map for irrigation was not presented in the study. *Chegbeleh et al. (2020)* and *Gidey (2018)* in separate studies also evaluated groundwater quality for mainly irrigation purposes but developed spatial thematic layers and suitability maps complementing the previous studies. This present study sought to evaluate the groundwater quality in the Savannah Region of Ghana, however, this study produced groundwater quality suitability maps for irrigation as well as finding the correlation between soil and groundwater quality which was lacking in the previous studies. This study, however, adopted an integrated approach combining statistical and geospatial methods to examine groundwater quality for irrigation purposes.

2. DESCRIPTION OF STUDY AREA

The study area comprises four districts, namely Karaga, Yunyoo-Nsuan, West Mamprusi, and Gushiegu district. The Upper East region borders the study area to the north, the Togo international border and Bunkurugu to the East, Kparigu to the East, and the Northern regions to the South as shown in *Figure 1*. The study region has a land area of about 5,282.9 km². The proximity of the Sahel and the Sahara winds makes the weather much drier in the northern sector than in the southern sectors. The rainy season lasts from May to October, with minimum temperatures ranging from 17 to 19 °C, and from December to February, the dry season starts, with temperatures ranging from 40 to 42 °C (*Adam & Appiah-Adjei 2019*). The area falls within the Voltaian basin (*Figure 1*). The lithological cover within this basin is unique and distinct compared to other areas. The most abundant geological unit in the study area is the Voltaian supergroup, which covers 74.2% of the study province and is typically made up of shale and mudstone with sandstone grit in small quantities (*Abdul et al. 2021*). The second abundant unit is the Panabako sandstone formation, which is also under the Voltaian supergroup and extends up to an area of about 14.3%, and is made up of cross-bedded quartz with intercalations of shale, mudstones, and siltstone

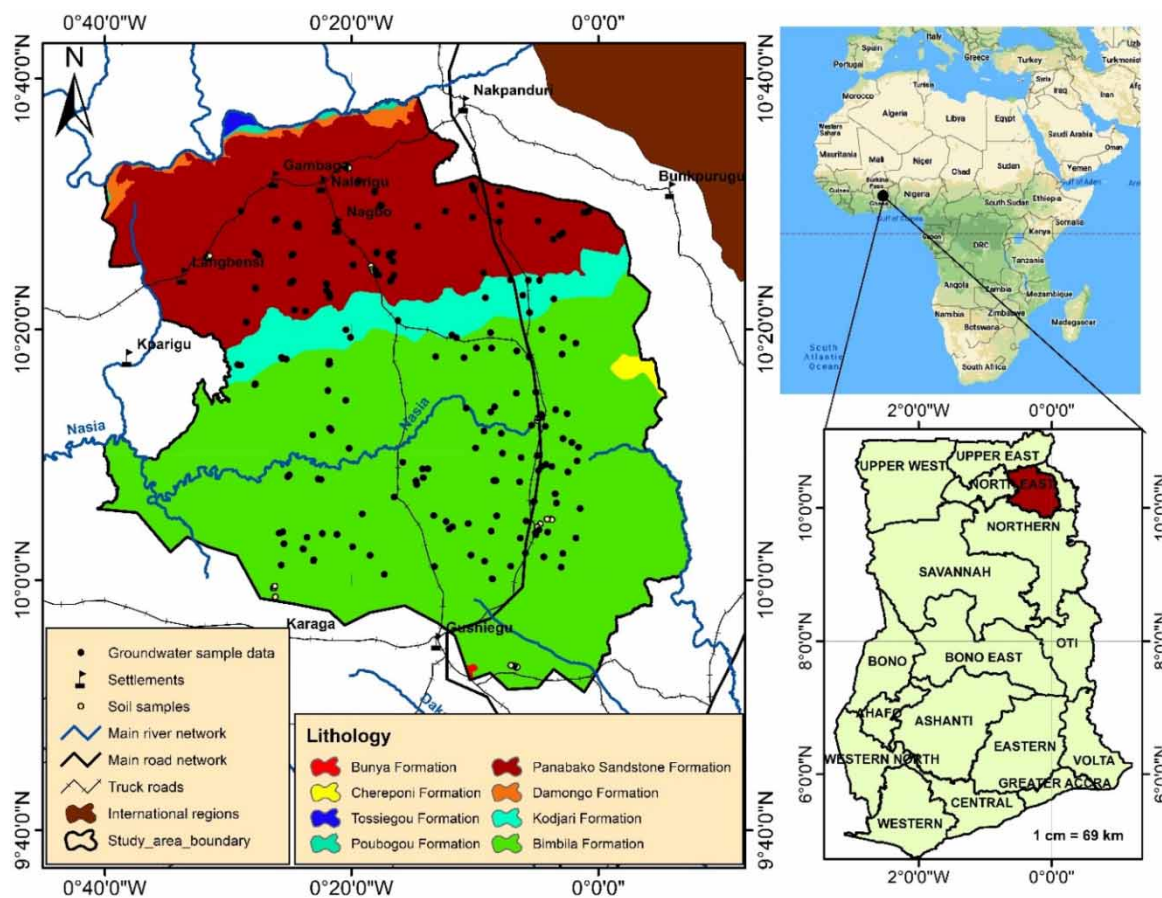


Figure 1 | Geographic location of the study area and sample points.

(Abdul-Rahaman *et al.* 2021). The Bunya and Poubogou formation constitutes sedimentary and metamorphic rocks but occupies only 7.9%.

3. MATERIALS AND METHODS

3.1. Sample collection and physiochemical analysis

Following the sampling protocols of Adimalla *et al.* (2020), groundwater samples were collected from 202 boreholes. The samples were collected from 2020 to 2021 during the dry season. The criteria were based on boreholes within the study region and hence boreholes outside the study area were not considered in this research. The samples were collected in acid-washed high-density linear polyethylene (HPDE) bottles of volume 1.5 l (a sample was taken from each borehole). They were filtered to remove contaminants using a Sartorius polycarbonate filtering apparatus and a 0.45 m cellulose acetate filter membrane. After filtration, the cation samples were immediately acidified to a pH < 2 with nitric acid, whereas the anion samples were not preserved. The Ion Balance Error (IBE) was adopted to perform the internal consistency test on the raw concentrations (Equation (1)). The IBE is the total cation concentration needed to balance the anions concentrations. The recognizable standard of IBE should be $\pm 5\%$ (Appelo & Postma 2005). Following this, any sample that did not reach the IBE norm of $\pm 5\%$ was eliminated for consideration in this study. Fortunately, all 202 groundwater samples came within the IBE's $\pm 5\%$ tolerance.

$$\text{IBE} = \frac{\sum \text{cations} - \sum \text{anions}}{\sum \text{cations} + \sum \text{anions}} \times 100 \quad (1)$$

where the ion concentrations are given in mEq/l.

The potential hydrogen (pH), electrical conductivity (EC), total dissolved solids (TDS), total hardness (TH), sodium (Na⁺), magnesium (Mg²⁺), potassium (K⁺), calcium (Ca²⁺), aluminum (Al³⁺), chloride (Cl⁻), sulfate (SO₄²⁻), carbonate (CO₃²⁻), sulfite (SO₃²⁻), nitrate (NO₃⁻), and bicarbonate (HCO₃⁻) are the groundwater quality parameters that were examined. Primarily, parameters like pH, EC, and TDS were measured using a pH meter, EC meter, and TDS meter, respectively. The amount of TH was determined by titration with the sodium salt of ethylenediaminetetraacetic acid (EDTA), and the detection was carried out with a Cu electrode. The cations were measured using an atomic absorption spectrophotometer (AAS), the anions were determined using an ultraviolet spectrophotometer (UV), and the bicarbonate concentration was measured using a titration process. Previous studies have used the same quality parameters to determine the suitability of groundwater for agriculture purposes (Anku *et al.* 2009; Yidana *et al.* 2012). Equations (2)–(6) were deployed to calculate irrigation water quality parameters.

$$\text{Sodium absorption ratio (SAR)} = \frac{\text{Na}^+}{\sqrt{\frac{1}{2} [\text{Ca}^{2+} + \text{Mg}^{2+}]}} \quad (2)$$

$$\text{Residual sodium carbonate (RSC)} = [\text{CO}_3^{2-} + \text{HCO}_3^-] - [\text{Ca}^{2+} + \text{Mg}^{2+}] \quad (3)$$

$$\text{Potential Salinity (PS)} = \text{Cl}^- + \sqrt{\text{SO}_4^{2-}} \quad (4)$$

$$\text{Kelly Ratio (KR)} = \frac{\text{Na}^+}{[\text{Ca}^{2+} + \text{Mg}^{2+}]} \quad (5)$$

$$\text{Magnesium Hazard (MH)} = \frac{\text{Mg}^+}{[\text{Ca}^{2+} + \text{Mg}^{2+}]} \times 100 \quad (6)$$

3.2. Soil sampling and analysis

From Figure 1, it was observed that soil samples were collected at random grids (farm sites, towns, and industrial areas) to assess the impact of soil properties on groundwater quality. A random sampling grid was produced for sampling using the grid tool in QGIS 3.26.2. Auger/chisel holes were dug at a depth of 25 cm. From Figure 1, the different sampling points are shown across the study area. The soil samples collected for laboratory analysis were

air-dried and sieved to pass through a 2-mm sieve. The soil pH was determined using a glass electrode at a soil-to-water ratio of 1:1 (Mclean 2015) at the Soil Laboratory at the University for Development Studies.

3.3. Spatial analysis of groundwater quality for irrigation

Several datasets were acquired to assess the impacts of surficial factors on groundwater quality for irrigation. These datasets include slope, geology, soil, and satellite imagery of the study area, except for the satellite imagery all other spatial datasets were acquired from the University for Development Studies Soil Laboratory. The datasets were provided in a vector format but were later rasterized in the GIS environment (QGIS) using the conversion tools.

3.4. Land use land cover classification

The first and most important pre-analysis procedures in using Landsat datasets are cloud cover, shadows, and no data removal. However, this study had a dataset with cloud cover ranging from 0 to 3%, therefore, doing this cloud cover removal was deemed unnecessary. The satellite imagery used for the land use land cover (LULC) was Landsat 8–9 (using bands 2, 3, 4, and 5). The QGIS 3.26.3 software program was used for the LULC, the essence of using this program was to produce a LULC map with higher spatial accuracy. The study employed the Random Forest (RF) algorithm which has been reported in recent studies to be higher performing compared to other classifiers like ISODATA and minimum distance (Naghibi *et al.* 2017; Kpiebaya *et al.* 2022). The putative land use type was selected using the Garmin 62s GPS device, and the selected coordinates were cross-referenced using Google Earth Pro data.

3.5. Geostatistical analysis of groundwater quality parameters

The difference between classical statistics and geostatistics is the assumption of spatial dependency. Several studies have adopted different interpolation methods to show the spatial distribution of groundwater parameters across the globe (Gidey 2018; Rawat *et al.* 2019). The essence of geospatial analysis is to visualize areas of low to high concentrations which might not be suitable for exploration purposes. Some of these interpolation methods used in previous studies include IDW (Inverse Distance Weight), Kriging, Zoning, and Spline. The smart-map plugin was activated in QGIS and selected groundwater quality parameters (EC, pH, TDS, SAR, MH, RSC, HCO₃⁻, PS, KR, TH, and Cl⁻) were interpolated using ordinary kriging. The main benefit of using kriging over alternative interpolations is that an un-sampled point attribute value is the weighted average of known values in the area, and the weights are proportional to the distances between the forecast site and the sampled locations (Zandi *et al.* 2011; Moharir *et al.* 2019). The main outputs from the analysis were the range, standard error, root mean square, partial sill, and lag size which are mathematically known and expressed in past and recent studies (Reza *et al.* 2017). The soil pH was also interpolated using geostatistics; however, the ‘Extract Multi Values to Points’ in the processing toolbox was used to extract the cell values from the soil pH layer and the groundwater pH layer for the statistical analysis.

3.6. Statistical analysis

The data obtained were first subjected to descriptive statistical analysis and variability expressed in terms of range, standard deviation, and coefficient of variation. Also, an analysis of variance (ANOVA) was conducted to assess the impact of soil pH on groundwater pH. The essence of these was based on the assumption that the study area had high groundwater pH, however, this was observed in agricultural areas and the relationship between soil pH and groundwater was considered prominent in this study. The groundwater parameters were selected to spatially determine the efficacy of groundwater quality for agriculture EC, pH, TDS, SAR, MH, RSC, HCO₃⁻, PS, KR, and TH. These parameters were selected with reference to Gidey (2018), Rawat *et al.* (2018), and Pandey *et al.* (2020). The selected parameters were exported from the kriged format to a GeoTIFF file showing areas of low and high variations.

The weight of each decisive factor is deduced from the optimum eigenvalue in the pairwise matrix as shown in Table 1. The key advantage of using the AHP method over other methods was its ability to study several parameters at multiple scales. Furthermore, it helps scientists to incorporate data from multiple criteria based on their relative weights, supported by expert knowledge, to create a single output map (Sapkota *et al.* 2021). The consistency ratio (CR), which must be less than or equal to 0.1, determines the validity. If it exceeds this threshold, it is recommended that the process be revised until a uniformity of 0.1 is attained; in this study, the

Table 1 | AHP ranking is used in assigning weights to the thematic layers in the overlay analysis

Factors	SAR	TDS	EC	MH	RSC	HCO ₃ ⁻	pH	PS	KR	Cl ⁻	NPE (%)	Weights
SAR	1.00	1.07	1.00	1.07	1.16	1.16	1.13	1.07	1.00	1.00	10.62	0.11
TDS	0.94	1.00	1.07	1.13	1.13	1.11	1.11	1.11	1.00	1.00	10.56	0.11
EC	1.00	0.94	1.00	1.13	1.13	1.13	1.07	1.13	1.00	1.00	10.51	0.11
MH	0.94	0.88	0.88	1.00	1.07	1.11	1.13	1.11	1.00	1.00	10.06	0.10
RSC	0.86	0.88	0.88	0.94	1.00	1.11	1.11	1.11	1.00	1.00	9.83	0.10
HCO ₃ ⁻	0.86	0.90	0.88	0.90	0.90	1.00	1.11	1.13	1.00	1.00	9.65	0.10
pH	0.88	0.90	0.94	0.88	0.90	0.90	1.00	1.13	1.00	1.00	9.52	0.10
PS	0.94	0.90	0.88	0.90	0.90	0.88	0.88	1.00	1.00	1.00	9.28	0.09
KR	1.00	1.00	1.00	1.00	1.00	1.00	1.00	1.00	1.00	1.00	9.99	0.10
Cl ⁻	1.00	1.00	1.00	1.00	1.00	1.00	1.00	1.00	1.00	1.00	9.99	0.10

NPE, Normalize Principal Eigenvector.

consistency was within a 0.1 limit. Equation (7) is used to calculate the CR.

$$CR = \frac{CI}{RI} \quad (7)$$

where RI is the random index and CI is the consistency index computed using Equation (8).

$$CI = \frac{\lambda_{\max} - n}{n - 1} \quad (8)$$

In this equation, λ is the matrix principal eigenvalue, and n is the number of factors used in the estimation (Saaty 1987). The groundwater quality index (GQI) was calculated using 10 spatial layers. This is accomplished using the weighted linear combination (WLC) proposed by Malczewski (1999), as shown in Equation (9).

$$GQI = m \sum_{j=1}^n 1(W_j \times X_i) \quad (9)$$

Here, GQI is the suitability index, X_i is the normalized weight of the i th feature of the thematic layer, W_j is the normalized weight of the j th thematic layer, m is the sum of themes, and n is the sum of classes in a theme. This trend, however, occurs in ArcGIS using the overlay tool, whereas Equation (4) is applicable in QGIS using the raster calculator. As shown in Table 1, SAR had the highest weight of 10.65% while PS had the lowest (9.28%).

4. RESULTS AND DISCUSSION

4.1. Physiochemical analysis

The essence of physiochemical parameters in this study cannot be underplayed because it is the primary determinant for drinking, domestic, agricultural, and industrial uses (Ewida *et al.* 2020). Presented in this study is a summary of physiochemical results depicting the chemical composition of groundwater in the study area. From Table 2, pH ranged from 5.69 to 8.89, with an average value of 8.06, indicating that the groundwater in the study area is slightly alkaline which agrees with the saline groundwater type in Abu Dhabi, UAE reported by Batarseh *et al.* (2021).

However, TDS in the study area ranged from 8.73 to 1,367.83 mg/l, with an average of 370.44 mg/l, it was found that 98.02% of the samples were within the acceptable limits (WHO). These results correspond to Ewida *et al.* (2020) because of similar geology. TH in groundwater samples in this study ranged from 0.49 to 267.50 mg/l. Sajil Kumar *et al.* (2014) reported some devastating effects of high TH in groundwater including; corrosiveness on metallic pipes and altering groundwater chemical composition. It was noticed that 73.27% of the analyzed samples in this study were within the acceptable WHO standards of TH (Table 2).

Na⁺ was found to be the dominant cation in the groundwater samples analyzed, ranging from 1.56 to 434.47 mg/l with a mean value of 110.52 mg/l (Table 2). The importance of Na⁺ in this study is equally important

Table 2 | Qualitative statistical analysis of groundwater samples

Quality parameters	Units	Min	Max	Mean	STD	CV	Acceptable limits	Number of qualified samples	Number of qualified samples (%)
pH		5.69	8.89	8.06	0.80	0.10	6.5–8.5	105	51.98
TDS	mg/l	8.73	1,367.83	370.44	250.27	0.68	1,000	198	98.02
EC	S/m	2.00	245.00	67.50	38.70	0.57	1,000	175	86.63
TH	mg/l	0.49	267.50	74.17	55.00	0.74	500	148	73.27
NO ₃ ⁻	mg/l	0.00	108.61	3.59	9.73	2.71	10	184	91.09
Cl ⁻	mg/l	0.89	747.53	33.29	80.81	2.43	250	197	97.52
SO ₄ ²⁻	mg/l	0.09	596.90	37.44	67.91	1.81	250	197	97.52
CO ₃ ²⁻	mg/l	0.00	21.00	4.39	4.80	1.09	200	202	100.00
HCO ₃ ⁻	mg/l	4.27	685.03	292.07	173.13	0.59	250	86	42.57
Na ⁺	mg/l	1.56	434.47	110.52	88.01	0.80	200	169	83.66
K ⁺	mg/l	1.25	59.35	8.00	7.03	0.88	30	200	99.01
Ca ²⁺	mg/l	0.04	102.52	15.68	14.73	0.94	200	202	100.00
Mg ²⁺	mg/l	0.01	27.95	6.14	6.86	1.12	70	202	100.00
SAR	mg/l	0.15	42.17	8.20	8.28	1.01	10–25	64	31.68
RSC	mg/l	3.00	656.21	274.65	175.31	0.64	125–250	47	23.27
PS	mg/l	1.39	749.35	38.07	81.26	2.13	4.23–8.23	18	8.91
KR		0.06	101.05	11.09	16.38	1.48	1	42	20.79
MH	%	0.46	60.00	24.97	13.78	0.55	50	194	96.04

STD, standard deviation; CV, coefficient of variation.

to other quality parameters but it is an essential parameter in computing SAR and KR. It was observed that 86.63% of samples analyzed for EC were within the desirable limits ranging from 2 to 245 mg/l. Continually, HCO₃⁻ was found to be within the range of 4.27 and 685.03 mg/l, with an average of 292.07 mg/l suggesting its adaptability for irrigation purposes. The wide variation in the physical parameters can mainly be attributed to the existing geology and climatic variation. Also, physical parameters are exacerbated by anthropogenic activities.

In the present study, Na⁺ > Ca²⁺ > K⁺ > Mg²⁺ was the major cation concentration in that order in the groundwater collected. However, the occurrence of Na⁺ in groundwater indicates the influence of sedimentary rocks such as sandstone on the aquifer (Singh *et al.* 2012). This is because sandstone contains high levels of salts and hence during the rainy season the dissolvable salts are then infiltrated into the aquifer through percolation. The occurrence of these cations in this study is consistent with studies of Yidana *et al.* (2012), and Yidana *et al.* (2013) because of the same study regime and methodology.

From Table 2, Cl⁻ was the major occurring anion (Cl⁻ > HCO₃⁻ > SO₄²⁻ > NO₃⁻ > CO₃²⁻) in the study area. The cation–anion interaction shows two major groundwater types, namely: low mineralized water (Mg²⁺–CO₃²⁻ and K⁺–SO₄²⁻) and high mineralized water (Na⁺–HCO₃⁻ and Ca²⁺–HCO₃⁻) which are consistent with results from the piper trilinear diagram. The essence of unearthing the groundwater type is to have a general perceptive of the influence of hydrogeochemical processes and anthropogenic activities on groundwater in the study area.

The results showed that high mineralized water (Na⁺–HCO₃⁻ and Ca²⁺–HCO₃⁻) can be attributed to the water–rock interactions, specifically weathering of aluminosilicates, dissolution of carbonate minerals, and cation exchange reactions within the Voltaian supergroup of the Bimbilla formation and the Panabako sandstone (Figure 1) (Yidana *et al.* 2012; Chegbeleh *et al.* 2020). In summary, 72.33% of the groundwater samples analyzed were within the desired quality requirements (WHO), implying that the groundwater in the study area is moderately suitable for both irrigations.

4.2. Impact of LULC on groundwater quality for irrigation

The influence of LULC in groundwater quality assessment cannot be undermined because it is a major determinant of the high concentration of some parameters. However, the recent global climatic issues have exacerbated the impact and led to poor quality. Several studies have reported the effects of LULC on groundwater potential

and quality across the globe, indicating that the high levels of some parameters can be linked to anthropogenic factors, climatic change variability, and land use change (Goyette *et al.* 2019; Yan *et al.* 2022). From the LULC statistics, shrublands had the largest area of about 46.96% and the least was the rivers which had an area of 0.02%. The codominant LULC classes were settlements, croplands, riparian, dams, open woodlands, and close woodland which had an area of 10.5, 5.68, 1.35, 0.34, 11.44, and 23.7%, respectively. Furthermore, analysis from the post-classification statistics yielded an overall accuracy (OV) of 94.27% which is recognized as a higher accuracy. Munyati (2019) in a study reported the accuracies of different classifiers and found RF to have an accuracy of 96% compared to Support Vector Machine (SVM) which had 93% indicating that RF is better performing.

Parameters (pH, TDS, and EC) that exceeded the desirable limits were superimposed on the LULC to uncover the relationship between them (Figure 2). Most of the parameters (salinity hazard) were abundant around croplands, settlements, and bare lands. The variations in these parameters leading to the high salinity can be attributed to the current farming practices and aridity in the study area. Abdul-Ganiyu *et al.* (2011) in a study reported findings on the high infiltration rate and the major farming system (rice farming) around the Nasia basin. The rice farms are found within the floodplains (riparian and along waterbodies) and this requires a large amount of inorganic fertilizers which directly and indirectly affects the groundwater quality. The high infiltration rates in the area make it easier for surface water and overbank flooding water to seep into the immediate groundwater reserve. Slabe-Erker *et al.* (2017) in a study appraised the impact of some agricultural practices on groundwater quality and findings from the study revealed high levels of nitrogen in the groundwater samples collected. The high level of EC can be attributed to the aridity in the study area because materials from soil and rocks are easily dissolved as water percolates downwards, leading to the high concentration of EC. Figure 2 indicates that shrublands are more dominant moving toward the northern sector of the study showing high levels of EC and pH.

From Table 3, $p = 0.02891$ (at $p < 0.05$) which shows a 2.9% probability of soil pH impacting groundwater quality (pH). Also, Table 4 presented $p = 0.044$ (at $p < 0.05$) suggesting a 4.4% chance of soil organic carbon and

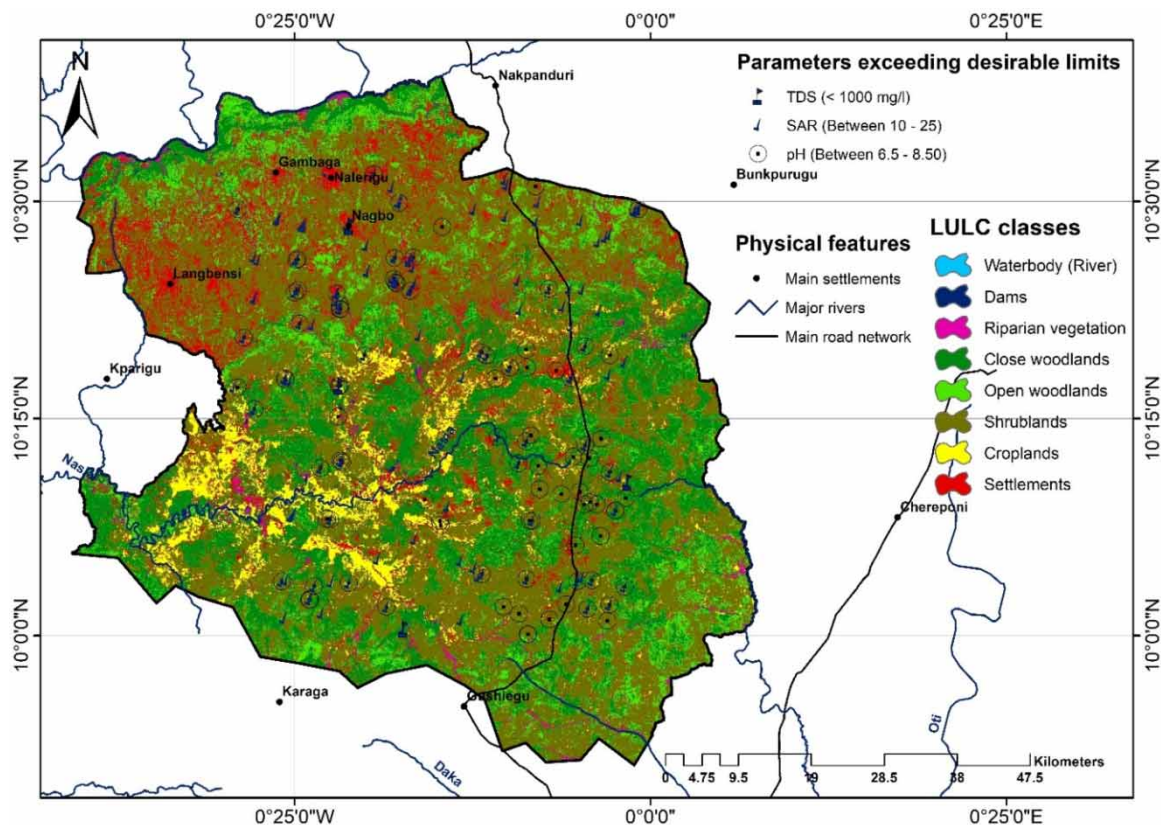


Figure 2 | LULC of the study area with some parameters exceeding the desirable limits.

Table 3 | ANOVA of groundwater pH and soil pH

Source of variation	SS	df	MS	F	P-value	F-crit
Between groups	1.808649	1	1.808649	4.988558	0.02891	3.986269
Within groups	23.92892	66	0.362559			
Total	25.73757	67				

SS, sum of squares; df, degree of freedom; MS, means of squares.

Table 4 | ANOVA of groundwater NO₃, soil organic matter (SOM), and soil organic matter (SOC)

Source of variation	SS	df	MS	F	P-value	F-crit
Between groups	43.00026	2	21.50013	3.116201	0.048702	3.08824
Within groups	683.0475	99	6.89947			
Total	726.0478	101				

SS, sum of squares; df, degree of freedom; MS, means of squares.

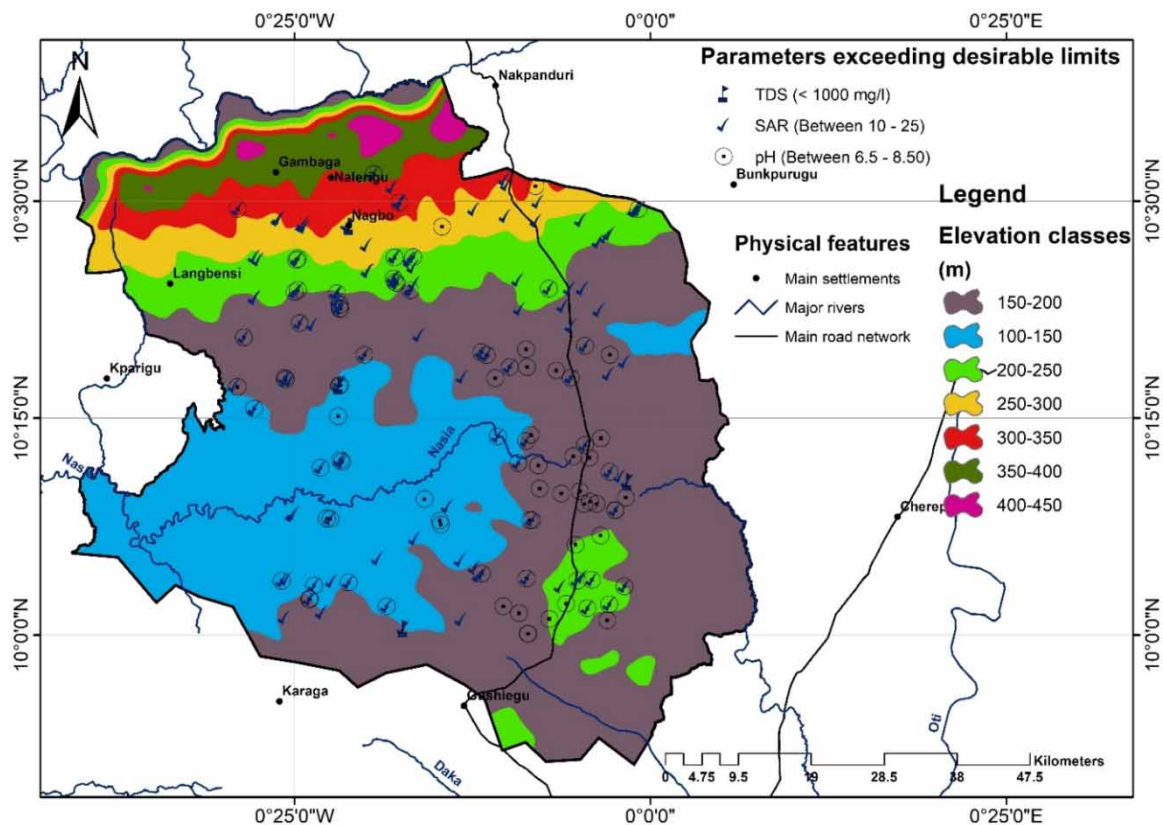


Figure 3 | Spatial variation of elevation in the study area.

organic matter influencing the concentration of nitrate in groundwater. The essence of adopting this statistical approach is to confirm findings from the spatial analysis as seen in the LULC map. This probability of groundwater pollution can mainly be attributed to the impact of land use activities in and partly spatio-temporal variation as reported in some studies (Alawi 2023; Shrestha & Shakya 2023).

4.3. Impact of elevation on groundwater quality

The quality of groundwater is dependent on elevation. However, limited studies have been done to unearth this phenomenon. The elevation in this study ranges from 150 to 450 m. Several studies have shown that areas with

high elevations are likely to have low groundwater occurrence compared to areas with low elevations (Fuentes *et al.* 2019; Naves *et al.* 2021). This is due to the predilection of gentle slopes holding rainfall for a period to facilitate groundwater recharge, whereas profound slopes will expedite runoff, most likely into zones of gentle slopes. Figure 3 shows that the gentle slope zones range from 150 to 250 m and it can be observed that these areas are consistent with the lowlands where rice farming occurs and regions of steep slopes ranging from 250 to 450 m. Also, the quality parameters exceeding desirable limits were found to be occurring around gentle sloping areas which are associated with croplands, shrublands, settlements, and bare lands. These lowlands are characterized by soils of alluvium deposits which are considered suitable for agricultural activities. This scenario is probabilistic to groundwater contamination because slopes serve as pathways for groundwater replenishment and therefore issues of rapid urbanization and industrialization may be contributing factors that may render it unsafe (Naves *et al.* 2021). In context, areas of low slopes are likely to have problems associated with poor quality while areas of high slopes may be ingestion points of contaminants into groundwater.

4.4. Spatial variability of groundwater quality parameters

From the spatial layers shown in Figure 4, pH, EC, and TDS had a direct correlation showing the same extent of variation. This is because the region of high pH is consistent with the region with high EC and TDS describing the salinity nature of the study area. The pH in the area ranges from 6.681 to 8.662 (Figure 4) which showed a higher concentration in the southern part of the study area while EC and TDS varied from 9.767 to 136.51 S/m and 54.409 to 662.827 mg/l. The high variation of pH, EC, and TDS trends affects the final suitability map for irrigation which may show the southern part of the study area as having poor groundwater quality. The high salinity hazard in the southern part may be attributed to land use activities like the intensive farming system in the study area practice in the dry and rainy seasons. Regarding the effects of bicarbonate hazard on soil and plants, a high concentration of RSC and HCO_3^- were observed around the central and southern parts of the study area. From the spatial analysis (Figure 4(e)–4(k)), RSC and HCO_3^- had values ranging from 52.45 to 491.79 mg/l and 33.76 to 502.163 mg/l, respectively. The high concentration of RSC in the southern part of the study area renders it unsafe for agricultural activities. In the framework of SAR and PS, the same variation was found with EC and pH as seen

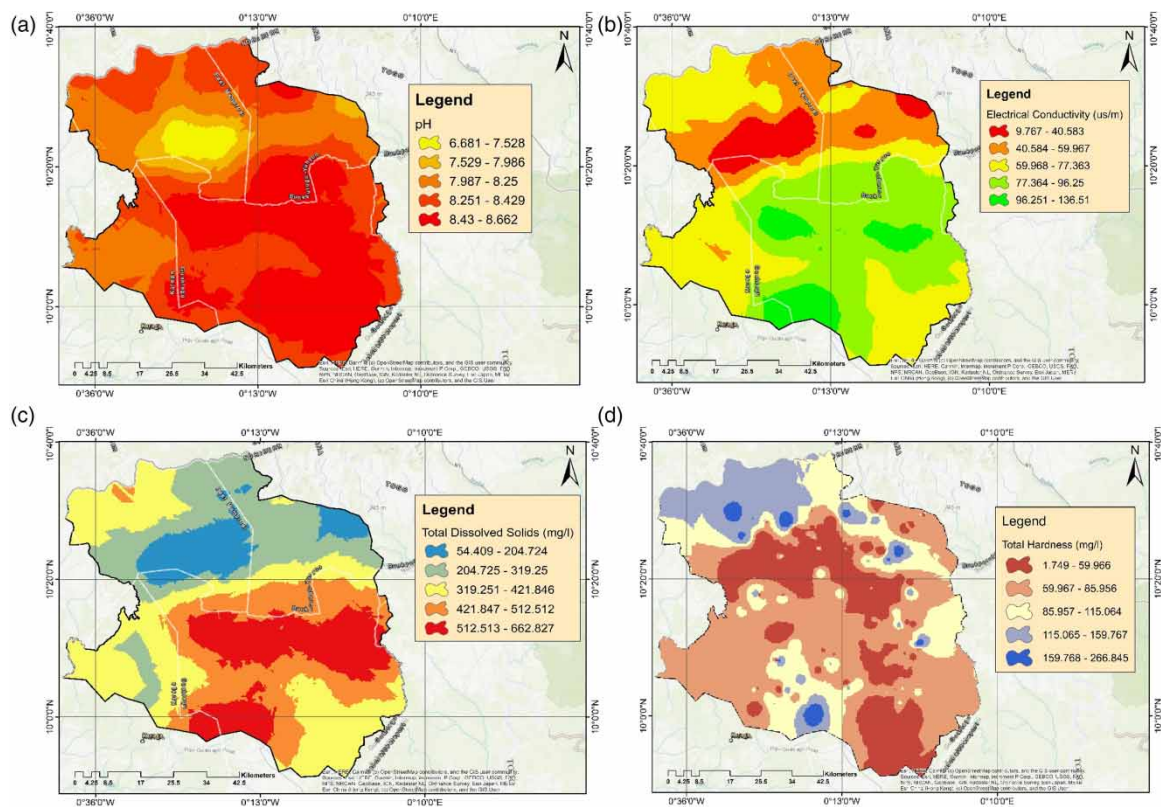


Figure 4 | Spatial variation of quality parameters: (a) pH; (b) EC; (c) TDS; (d) TH; (e) RSC; (f) SAR; (g) PS; (h) MH; (i) KR; (j) Cl^- ; and (k) HCO_3^- . (continued).

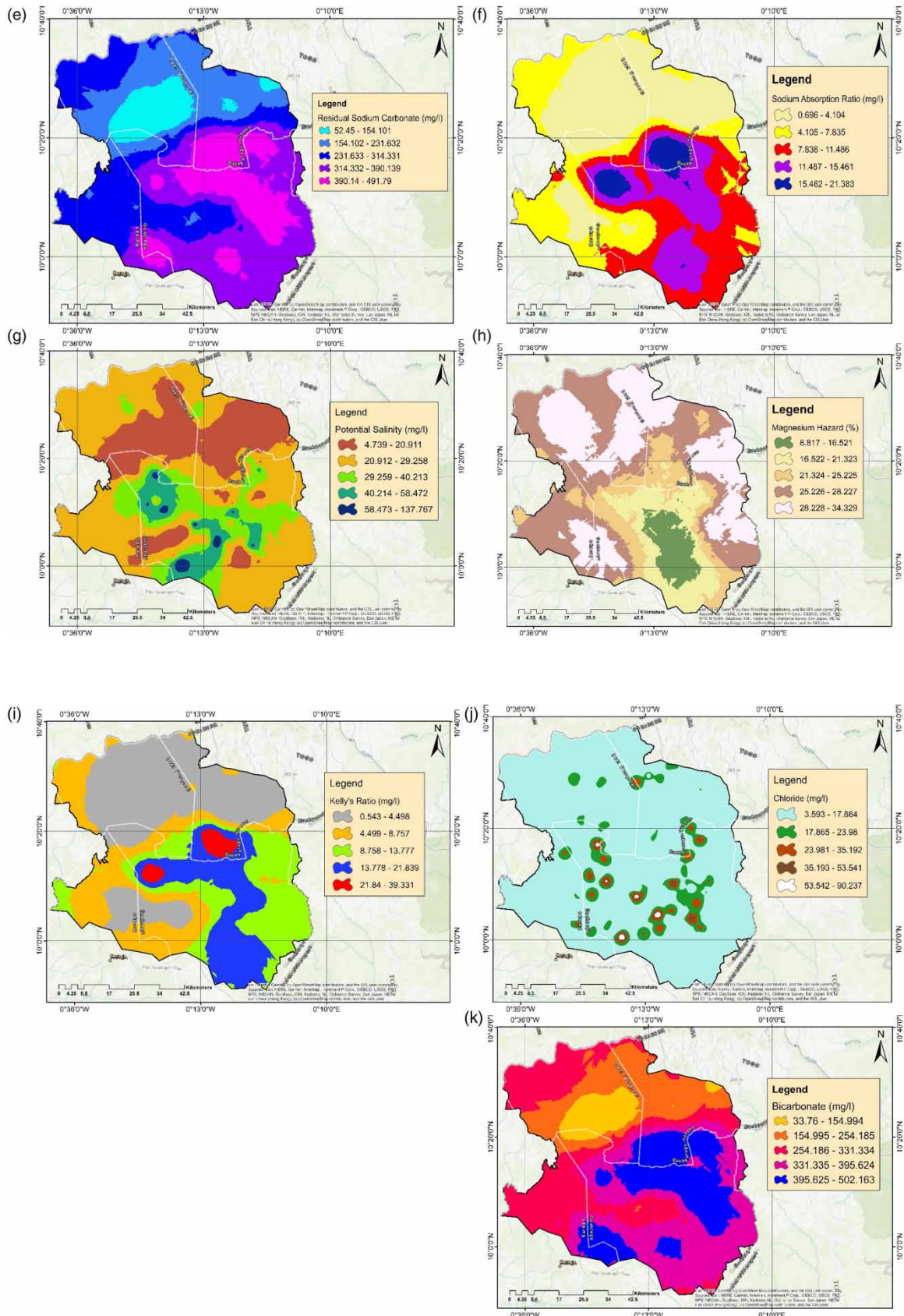


Figure 4 | Continued.

in the southern part of the study region. The major finding from the spatial analysis is consistent with the final suitability map showing that the southern parts have poor groundwater quality for irrigation.

4.5. Spatial suitability of groundwater quality for irrigation use

The AHP rankings reveal that SAR had the highest weight of 10.62% and the lowest weight was PS with 9.28%. This is because of SAR's impact on agriculture; however, the assigned weights were not very distinct from each other. The difference between the highest and the lowest weight was 1.34% indicating the importance and impact of all the thematic layers. Groundwater quality for irrigation in the study area was classified into three classes: good quality, moderate quality, and poor quality (Figure 5). The regions that were found to have good groundwater quality for irrigation had an area of 1,534.34 km², areas of moderate groundwater quality had an area of 1,933.35 km², and poor quality for irrigation covered an area of 1,815.21 km². Some of the quality parameters (SAR, TDS, and pH) that exceeded the permissible limits were abundant around regions of good quality for irrigation. This is because more quality parameters were used in the model with varying weights and may have compensated for the high salinity around these areas. Also, the high SAR values for these areas were less than half samples and hence the remaining half may have also compensated for the undesired samples rendering these areas safe for agricultural activities. It is vital to note that about 1,815.21 km² of the study area was found to be poor quality for irrigation which is worrisome for agricultural productivity. Most of these areas are consistent with the lowlands where rice farms are located. The main reason for this can be attributed to the high concentration of bicarbonate and pH which are a result of land use activities in the study area. Also, lowlands are zones of groundwater recharge and hence can easily be pollution zones depending on specific anthropogenic activities. Also, in the context of overbank flooding of rivers pH, OM, and OC are carried far away from the source and deposited at discharge zones, and hence the boundaries between moderate and poor zones are influenced by distance from the river as seen around the Nasia River (Figure 5).

The essence of this analysis is to inform irrigators and agriculturists about areas wholesome for exploration for agricultural purposes. Analysis from this study is similar and consistent with studies of [Rakotondrabe et al. \(2018\)](#) in East Cameroon around a mining site, which found groundwater quality favorable for irrigation. Findings from

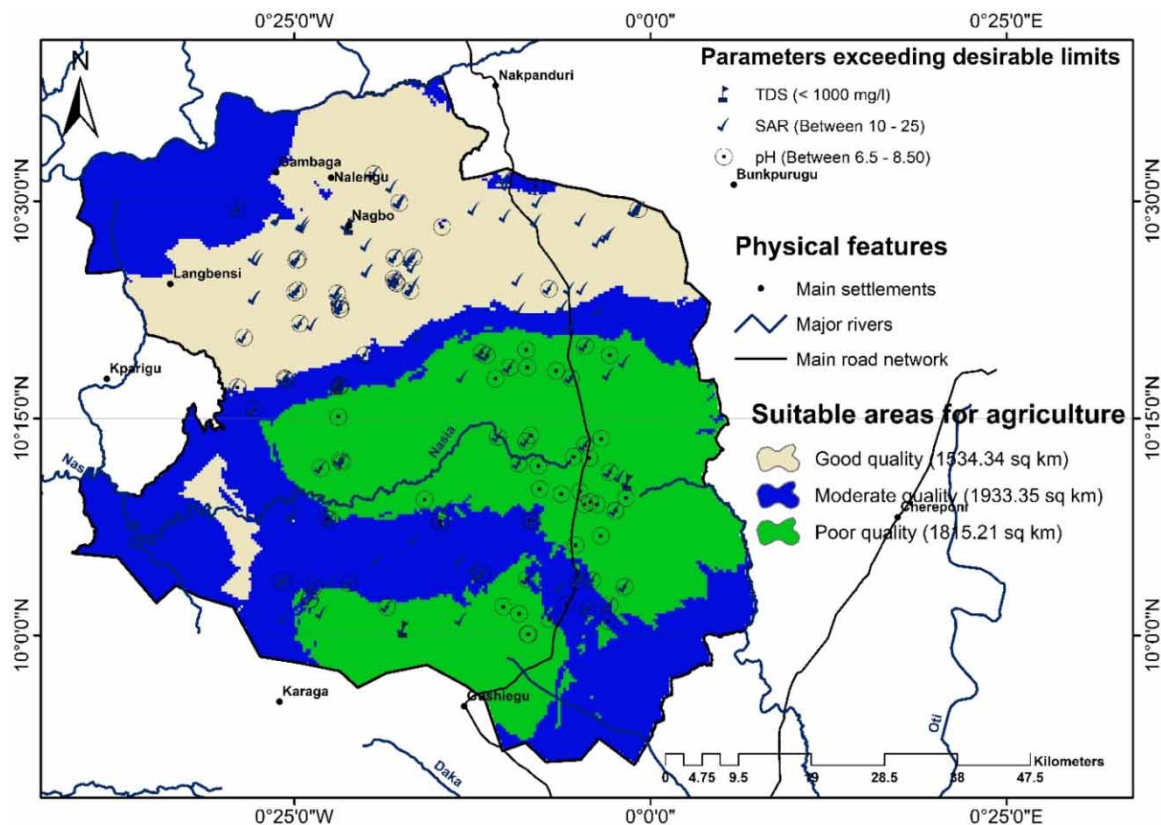


Figure 5 | Groundwater quality for irrigation in the study area.

the studies revealed that groundwater quality around the surrounding communities can be explored for irrigation because the largest classes were found to have good quality and the least was found to be very close to the mines. However, studies by [Rakotondrabe *et al.* \(2018\)](#) conflict results reported by [Semy & Romeo \(2021\)](#) who found mining communities to have poor water quality for irrigation, this can be attributed to the type of mining and processes involved. The main finding from this work showed that more than 3,467.69 km² of the entire study area have groundwater quality useful for irrigation and the remaining 1,815.21 km² should be given more attention to reducing the possible effect on irrigation as seen in [Figure 5](#).

4.6. Hydro-chemical facies (piper trilinear analysis)

Three main types of groundwater were found in the study area each of which exists in different combinations ([Figure 6](#)). The first groundwater type in the study area was found to be Na–HCO₃, the second was an intermediate type containing both Na–Ca–HCO₃, and the third water type is Ca–HCO₃. These groundwater types tend to raise the pH levels which can cause havoc to soil and plants. From [Figure 4](#), it was observed that the bicarbonate concentration in the groundwater was extremely high, and about half of the samples were found to be unworthy. The results suggest that bicarbonate should be given more attention when used in the cultivation of fruits and vegetables. These findings are also in accordance with studies reported by [Moharir *et al.* \(2019\)](#) and [Krishna Kumar *et al.* \(2014\)](#) who found the main groundwater type ranged between Na–HCO₃ to Ca–HCO₃. The similarities in findings can be fundamentally associated with the geology type in the coastal area of South Chennai, India, and Mahoba, Uttar Pradesh in India similar to the geology type in [Figure 1](#). However, these studies have reported that groundwater of these types usually has good quality for irrigation purposes.

4.6. Spatial dependence of groundwater quality parameters (cross-validation)

Geostatistics is an important spatial tool that has been used in recent years to evaluate groundwater quality for different purposes by unearthing the spatial structure of these parameters. The best-fit model used in this study is depicted in the Supplementary data ([Figure S1\(a\)–1\(k\)](#)). Five different isotropic semivariogram models were used,

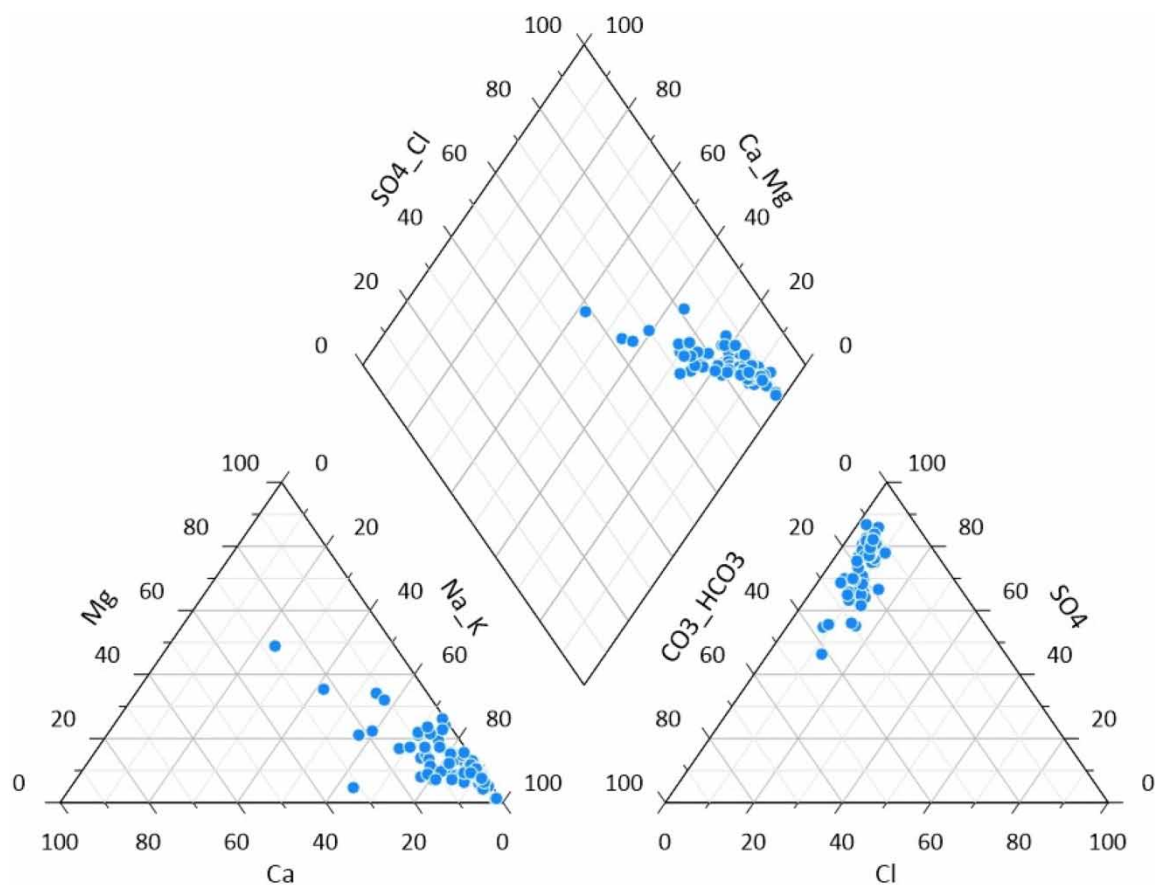


Figure 6 | Piper plot showing the different groundwater types in the study area.

Table 5 | Best-fit model summary of semivariogram analysis for groundwater quality parameters

Parameter	Model	Nugget	Range	Partial sill	Lag SIZE	Mean	RMS	RMSE	Regression equation $Y = mx + c$
EC	Stable	0.379	0.320	0.750	0.027	-0.035	29.208	1.139	$0.57x + 27.92$
TDS	Gaussian	0.486	0.265	0.620	0.025	1.660	191.350	1.061	$0.53x + 171.56$
SAR	Stable	0.285	0.322	1.046	0.027	-0.178	6.245	1.195	$0.57x + 3.412$
MH	Circular	0.795	0.286	0.272	0.024	-0.405	12.829	0.978	$0.17x + 20.56$
RSC	Circular	0.417	0.356	0.847	0.030	-0.347	128.800	1.011	$0.57x + 115.83$
HCO ₃	Circular	0.444	0.272	0.628	0.027	-2.449	130.010	0.985	$0.54x + 130.73$
pH	Spherical	0.479	0.292	0.609	0.024	0.016	0.623	0.991	$0.40x + 4.866$
PS	Stable	0.379	0.198	0.646	0.017	-3.206	75.299	1.088	$0.1x + 27.77$
KR	Spherical	0.339	0.293	0.790	0.032	-0.367	13.800	1.245	$0.32x + 6.034$
TH	K-Bessel	0.035	0.002	1.183	0.0002	-0.750	53.770	0.935	$0.007x + 74.32$
Cl	Stable	0.504	0.025	0.431	0.012	-5.614	74.986	1.143	$0.027x + 23.32$

namely Stable, Circular, Spherical, Gaussian, and K-Bessel (Table 5). The isotropic models were chosen because the spatial interdependence among variables developed in the same way in all orientations. The root mean squared error (RMSE) and root mean squared standardized error (RMSS) were used to validate spatial layers used in the overlay analysis (Clark 2010) study showed that the higher the nugget value (between 0 and 1) the smoother and more accurate the spatial layer. The higher nugget value was 0.795 (circular model) which was used to develop the MH layer, suggesting a smoother layer compared to TH (K-Bessel) with 0.035. This study showed that the Stable, Gaussian, Circular, and Spherical semivariations were the best-fit semivariation. Also, RMSE has reported in several studies that it should be close to 1 to exhibit a higher accuracy (Setianto & Triandini 2015). The presented results showed that all quality parameters were close to 1 as seen in Table 5 indicating higher spatial dependent layers that can be used for further analysis.

5. CONCLUSION

Groundwater has special economic significance globally and locally because it is the largest hydro-structure with freshwater. Groundwater plays an important role in the supply of freshwater for domestic and agricultural use in rural communities around the world. Based on the analyzed samples, it can be concluded that the range of physiochemical parameters was within the acceptable limits for irrigation and therefore can be adopted for these purposes. The output from the overlay analysis showed that regions of good groundwater quality for irrigation had a total area of 1,534.34 km². Regions of moderate groundwater quality for irrigation had an area of 1,933.35 km² while zones of poor quality were found to be 1,815.21 km². Based on these findings, it is recommended that:

- Groundwater in the study area showed a degree of viability for agricultural purposes based on the analyzed samples. However, it is essential to subject future water samples to thorough quality analysis before use.
- Further research should be done to reveal the extent of the impact of LULC and some surficial factors on the groundwater. This will aid policymakers to develop strategies to combat and reveal groundwater pollution.
- The irrigation water requirements for crops should be strictly adhered to in order to avoid over-irrigation and subjecting crops to excess leaching of available nutrients. Also, agroforestry methods should be practiced within farmland to reduce the effect of aridity on crop production.
- Groundwater exploration is an expensive commodity in SSA, hence thorough geospatial modeling should be done in examining suitable areas for irrigation. Some of these models include artificial intelligence, deep learning, fuzzy overlay, machine learning, and many more.

ACKNOWLEDGEMENTS

Much gratitude to all of our colleagues who advised us on how to modify and remodel this research so that it could be published today. We would like to express our appreciation to the anonymous editor and reviewers

for their invaluable contributions to this paper. The opinions expressed in this paper do not necessarily reflect the views of the University for Development Studies (UDS).

DATA AVAILABILITY STATEMENT

Data cannot be made publicly available; readers should contact the corresponding author for details.

CONFLICT OF INTEREST

The authors declare there is no conflict.

REFERENCES

- Abdul, R. M., Arhin, E., Adjei, A., Jnr, A., Abdul, R. M. & Arhin, E. 2021 Mineralogy and geochemistry of geophagic materials at Mfensi-Adankwame in the Ashanti region of Ghana and possible health implications of the ashanti region of Ghana and possible health implications. *Geology, Ecology, and Landscapes* **00** (00), 1–12. <https://doi.org/10.1080/24749508.2021.1952775>.
- Abdul-Ganiyu, S., Kyei-Baffour, N. & Gbedzi, V. D. 2011 Analysis of some hydrological parameters of the nasia river catchment in the Northern Region of Ghana for its socio-economic development. *African Journal of Agricultural Research* **6** (24), 5533–5540. <https://doi.org/10.5897/AJAR11.423>.
- Abdul-Ganiyu, S. & Prosper, K. 2021 Estimating the groundwater storage for future irrigation schemes. *Water Supply* 1–15. <https://doi.org/10.2166/ws.2021.041>.
- Adam, A. B. & Appiah-Adjei, E. K. 2019 Groundwater potential for irrigation in the Nabogo basin, Northern Region of Ghana. *Groundwater for Sustainable Development* **9** (August), 100274. <https://doi.org/10.1016/j.gsd.2019.100274>.
- Adimalla, N., Dhakate, R., Kasarla, A. & Taloor, A. K. 2020 Appraisal of groundwater quality for drinking and irrigation purposes in Central Telangana, India. *Groundwater for Sustainable Development* **10**, 100334. <https://doi.org/10.1016/j.gsd.2020.100334>.
- Alawi, S. A. 2023 Evaluation of land use/land cover datasets in hydrological modelling using the SWAT model Sayed Amir Alawi. **6** (1), 63–74. <https://doi.org/10.2166/h2oj.2023.062>.
- Anku, Y. S., Banoeng-Yakubo, B., Asiedu, D. K. & Yidana, S. M. 2009 Water quality analysis of groundwater in crystalline basement rocks, Northern Ghana. *Environmental Geology* **58** (5), 989–997. <https://doi.org/10.1007/s00254-008-1578-4>.
- Appelo, C. A. J. & Postma, D. 2005 Geochemistry. *Groundwater and pollution* **536** (10.1201), 9781439833544.
- Batarseh, M., Imreizeeq, E., Tilev, S., Al Alaween, M., Suleiman, W., Al Remeithi, A. M., Al Tamimi, M. K. & Al Alawneh, M. 2021 Assessment of groundwater quality for irrigation in the arid regions using irrigation water quality index (IWQI) and GIS-Zoning maps: mirate, UAECASE study from Abu Dhabi E. *Groundwater for Sustainable Development* **14**, 100611. <https://doi.org/10.1016/j.gsd.2021.100611>.
- Chegbeleh, L. P., Akurugu, B. A. & Yidana, S. M. 2020 Assessment of groundwater quality in the Talensi District, Northern Ghana. *Scientific World Journal* **2020**. <https://doi.org/10.1155/2020/8450860>.
- Clark, I. 2010 Statistics or geostatistics? sampling error or nugget effect? *Journal of the Southern African Institute of Mining and Metallurgy* **110** (6), 307–312.
- Ewida, A. Y. I., Khalil, M. & Ammar, A. 2020 Impact of domestic wastewater treatment plants on the quality of shallow groundwater in Qalyubia, Egypt; discrimination of microbial contamination source using BOX-PCR. *Egyptian Journal of Botany* **0** (0), 0–0. <https://doi.org/10.21608/ejbo.2020.30986.1505>.
- Fuentes, I., Padarian, J., van Ogtrop, F. & Vervoort, R. W. 2019 Comparison of surface water volume estimation methodologies that couple surface reflectance data and digital terrain models. *Water* **11** (4), 780. <https://doi.org/10.3390/w11040780>.
- Gidey, A. 2018 Geospatial distribution modeling and determining suitability of groundwater quality for irrigation purpose using geospatial methods and water quality index (WQI) in Northern Ethiopia. *Applied Water Science* **8** (3), 1–16. <https://doi.org/10.1007/s13201-018-0722-x>.
- Giordano, M. 2006 Agricultural groundwater use and rural livelihoods in sub-Saharan Africa: a first-cut assessment. *Hydrogeology Journal* **14** (3), 310–318. <https://doi.org/10.1007/s10040-005-0479-9>.
- Goyette, J. O., Bennett, E. M. & Maranger, R. 2019 Differential influence of landscape features and climate on nitrogen and phosphorus transport throughout the watershed. *Biogeochemistry* **142** (1), 155–174. <https://doi.org/10.1007/s10533-018-0526-y>.
- Havril, T., Tóth, Á., Molson, J. W., Galsa, A. & Mádl-Szőnyi, J. 2018 Impacts of predicted climate change on groundwater flow systems: can wetlands disappear due to recharge reduction? *Journal of Hydrology* **563**, 1169–1180. <https://doi.org/10.1016/j.jhydrol.2017.09.020>.
- Kpiebaya, P., Ebo, E., Amuah, Y., Shaibu, A., Baatuuwie, B. N., Avorny, V. K. & Wullobayi, B. 2022 Spatial assessment of groundwater potential using quantum GIS and multi-criteria decision analysis (QGIS-AHP) in the Sawla-Tuna-Kalba district of Ghana. *Journal of Hydrology: Regional Studies* **43** (August), 101197. <https://doi.org/10.1016/j.ejrh.2022.101197>.
- Krishna Kumar, S., Bharani, R., Magesh, N. S., Godson, P. S. & Chandrasekar, N. 2014 Hydrogeochemistry and groundwater quality appraisal of part of south Chennai coastal aquifers, Tamil Nadu, India using WQI and fuzzy logic method. *Applied Water Science* **4**, 341–350.

- Malczewski, J. 1999 Visualization in multicriteria spatial decision support systems. *Geomatica* **53** (2), 139–147.
- Mclean, E. O. 2015 *Soil pH and Lime Requirement*, pp. 199–224. <https://doi.org/10.2134/agronmonogr9.2.2ed.c12>
- Moharir, K., Pande, C., Singh, S. K., Choudhari, P., Kishan, R. & Jeyakumar, L. 2019 Spatial interpolation approach-based appraisal of groundwater quality of arid regions. *Journal of Water Supply: Research and Technology – AQUA* **68** (6), 431–447. <https://doi.org/10.2166/AQUA.2019.026>.
- Munyati, C. 2019 Comparative performance of regression tree and parametric classification of savannah woody cover on SPOT 6 NAOMI imagery. *Remote Sensing Applications: Society and Environment* **13**, 171–182. <https://doi.org/10.1016/J.RSASE.2018.10.015>.
- Naghibi, S. A., Ahmadi, K. & Daneshi, A. 2017 Application of support vector machine, random forest, and genetic algorithm optimized random forest models in groundwater potential mapping. *Water Resources Management* **31** (9), 2761–2775. <https://doi.org/10.1007/s11269-017-1660-3>.
- Naves, A., Samper, J., Pisani, B., Mon, A., Dafonte, J. & Montenegro, L. 2021 Hydrogeology and groundwater management in a coastal granitic area with steep slopes in Galicia (Spain). *Hydrogeology Journal* **29** (8), 2655–2669.
- Pandey, H. K., Tiwari, V., Kumar, S., Yadav, A. & Srivastava, S. K. 2020 Groundwater quality assessment of allahabad smart city using GIS and water quality index. *Sustainable Water Resources Management* **6** (2). <https://doi.org/10.1007/s40899-020-00375-x>.
- Rakotondrabe, F., Ndam Ngoupayou, J. R., Mfonka, Z., Rasolomanana, E. H., Nyangono Abolo, A. J. & Ako Ako, A. 2018 Water quality assessment in the Bétaré-Oya gold mining area (East-Cameroon): multivariate statistical analysis approach. *Science of the Total Environment* **610–611** (May 2018), 831–844. <https://doi.org/10.1016/j.scitotenv.2017.08.080>.
- Rawat, K. S., Singh, S. K. & Gautam, S. K. 2018 Assessment of groundwater quality for irrigation use: a peninsular case study. *Applied Water Science* **8** (8), 1–24. <https://doi.org/10.1007/s13201-018-0866-8>.
- Rawat, K. S., Jeyakumar, L., Singh, S. K. & Tripathi, V. K. 2019 Appraisal of groundwater with special reference to nitrate using statistical index approach. *Groundwater for Sustainable Development* **8**, 49–58. <https://doi.org/10.1016/J.GSD.2018.07.006>.
- Reza, S. K., Nayak, D. C., Mukhopadhyay, S., Chattopadhyay, T. & Singh, S. K. 2017 Characterizing spatial variability of soil properties in alluvial soils of India using geostatistics and geographical information system. *Archives of Agronomy and Soil Science* **63** (11), 1489–1498. <https://doi.org/10.1080/03650340.2017.1296134>.
- Saaty, R. W. 1987 The analytic hierarchy process—what it is and how it is used? *Mathematical Modelling* **9** (3–5), 161–176.
- Sajil Kumar, P. J., Elango, L. & James, E. J. 2014 Assessment of hydrochemistry and groundwater quality in the coastal area of south chennai, India. *Arabian Journal of Geosciences* **7** (7), 2641–2653. <https://doi.org/10.1007/s12517-013-0940-3>.
- Sapkota, S., Pandey, V. P., Bhattarai, U., Panday, S., Shrestha, S. R. & Maharjan, S. B. 2021 Groundwater potential assessment using an integrated AHP-driven geospatial and field exploration approach applied to a hard-rock aquifer Himalayan watershed. *Journal of Hydrology: Regional Studies* **37** (September), 100914. <https://doi.org/10.1016/j.ejrh.2021.100914>.
- Semy, K. & Romeo, M. 2021 Quality assessment of Tsurang River water affected by coal mining along the Tsurangkong Range, Nagaland, India. *Applied Water Science* **11** (7), 1–11. <https://doi.org/10.1007/s13201-021-01444-y>.
- Setianto, A. & Triandini, T. 2015 Comparison of kriging and Inverse Distance Weighted (Idw) interpolation methods in lineament extraction and analysis. *Journal of Applied Geology* **5** (1), 21–29. <https://doi.org/10.22146/jag.7204>.
- Shrestha, G. & Shakya, B. M. 2023 Water infiltration rate in the Kathmandu Valley of Nepal amidst present urbanization and land-use change. **6** (1), 1–14. <https://doi.org/10.2166/h2oj.2023.044>.
- Singh, V. K., Bikundia, D. S., Sarswat, A. & Mohan, D. 2012 Groundwater quality assessment in the village of Lutfullapur Nawada, Loni, District Ghaziabad, Uttar Pradesh, India. *Environmental Monitoring and Assessment* **184** (7), 4473–4488. <https://doi.org/10.1007/s10661-011-2279-0>.
- Slabe-Erker, R., Bartolj, T., Ogorevc, M., Kavaš, D. & Koman, K. 2017 The impacts of agricultural payments on groundwater quality: spatial analysis on the case of Slovenia. *Ecological Indicators* **73**, 338–344. <https://doi.org/10.1016/j.ecolind.2016.09.048>.
- Yan, J., Chen, J. & Zhang, W. 2022 Impact of land use and cover on shallow groundwater quality in Songyuan city, China: a multivariate statistical analysis. *Environmental Pollution* **307** (May), 119532. <https://doi.org/10.1016/j.envpol.2022.119532>.
- Yidana, S. M., Banoeng-Yakubo, B., Aliou, A. S. & Akabzaa, T. M. 2012 Qualité des eaux souterraines des aquifères voltaïque et birimien du nord Ghana – application de méthodes statistiques multivariées et de systèmes d'information géographique. *Hydrological Sciences Journal* **57** (6), 1168–1183. <https://doi.org/10.1080/02626667.2012.693612>.
- Yidana, S. M., Fynn, O. F., Chegbeleh, L. P., Nude, P. M. & Asiedu, D. K. 2013 Hydrogeological conditions of a crystalline aquifer: simulation of optimal abstraction rates under scenarios of reduced recharge. *The Scientific World Journal* **2013**. <https://doi.org/10.1155/2013/606375>.
- Zandi, S., Ghobakhlou, A. & Sallis, P. 2011 Evaluation of spatial interpolation techniques for mapping soil pH. In: *MODSIM 2011 - 19th International Congress on Modelling and Simulation – Sustaining Our Future: Understanding and Living with Uncertainty*, December. pp. 1153–1159. <https://doi.org/10.36334/modsim.2011.c2.zandi>.

First received 24 March 2023; accepted in revised form 8 June 2023. Available online 7 July 2023